Talanta 89 (2012) 246–252

Contents lists available at SciVerse ScienceDirect

Talanta

journal homepage: www.elsevier.com/locate/talanta

Development of label-free optical diagnosis for sensitive detection of influenza virus with genetically engineered fusion protein

Tae Jung Park[a,b,*], Seok Jae Lee[b], Do-Kyun Kim[a], Nam Su Heo[a], Jung Youn Park[c], Sang Yup Lee[a,d,*]

[a] BioProcess Engineering Research Center, KAIST, 291 Daehak-ro, Yuseong-gu, Daejeon 305-701, Republic of Korea
[b] Center for Nanobio Integration & Convergence Engineering, National Nanofab Center, 291 Daehak-ro, Yuseong-gu, Daejeon 305-806, Republic of Korea
[c] Biotechnology Research Division, National Fisheries Research & Development Institute (NFRDI), 408-1 Sirang-ri, Gijang, Busan 619-705, Republic of Korea
[d] Department of Chemical & Biomolecular Engineering (BK21 program), Department of Bio & Brain Engineering, Department of Biological Sciences, and Bioinformatics Research Center, Center for Systems & Synthetic Biotechnology, and Institute for the BioCentury, KAIST, 291 Daehak-ro, Yuseong-gu, Daejeon 305-701, Republic of Korea

ARTICLE INFO

Article history:
Received 22 November 2011
Received in revised form 6 December 2011
Accepted 7 December 2011
Available online 27 December 2011

Keywords:
Surface plasmon resonance
Localized surface plasmon resonance
Biosensor
Influenza B virus
Gold-binding polypeptide
Fusion protein

ABSTRACT

An active immobilization method utilizing the metal-binding property was developed and examined for its ability to facilitate the biosensing of avian influenza virus. The special biosensing performance with optical plasmonic analysis, including surface plasmon resonance (SPR) was evaluated on gold substrate and also by SPR imaging (SPRi) and localized SPR (LSPR) system where antigen–antibody interaction occurs. A complete optical analytical system was developed by integrating microarray and fabricating nanoparticles onto a single glass chip, thus allowing specific and sensitive diagnosis with subsequent binding. Reaction condition for the maximum reactivity was optimized by SPR analysis and more sensitive interaction was performed by SPRi analysis. Furthermore, ultra-sensitive detection was successfully developed up to the target molecules of 1 pg mL^{-1} by LSPR analysis. The advanced phase-in of enhanced plasmonic sensing system allows more efficient and sensitive detection by switching fabrication processes, which were prepared on the gold surface using the nanoparticles. This inflow contains the gold binding polypeptide (GBP)–fusion protein, which was expressed in recombinant *Escherichia coli* cells, was bound onto the gold substrates by means of specific interaction. The GBP–fusion method allows immobilization of proteins in bioactive forms onto the gold surface without surface modification suitable for studying antigen–antibody interaction. It was used for the detection of influenza virus, an infectious viral disease, as an example case.

1. Introduction

Various valuable real-time tools, *in situ* analysis of dynamic surface events, have been developed for studying biomolecular interactions on the ultra-thin films [1–3]. Aside from the design of label and probes, active areas of research include an advanced method such as time-resolved or spatially resolved, evanescent wave, laser-assisted spectroscopy, surface plasmon resonance (SPR), and multidimensional data-acquisition [4–8]. Among them, SPR sensor system offers the advantages of label-free, rapid response time, highly sensitive and real-time detection of binding events between biomolecules [1–5]. Unfortunately, conventional SPR reflectometry sensor requires sophisticated optical instrumentation associated with the detection system. This limitation is significant, because biosensors are urgently in demand for high-throughput and cost-effective monitoring. For the enhancing the detection sensitivity, fiber bundle also has been employed for purposes of imaging or for biosensor array in recent years [3–8]. Fiber optic sensors are based on either direct or indirect (indicator-based) sensing schemes. In the first, the intrinsic optical properties of the analysis must be measured, for example its refractive index, absorption, or emission. In the second, the color or fluorescence of an immobilized indicator, label, or any other optically detectable bioprobe have to be monitored. The success of SPR in general and in the form of fiber-optic sensors, in particular, is impressive.

To overcome the limit of detections, we evaluated a SPR, SPR imaging (SPRi)- and localized SPR (LSPR)-based optical biosensor for label-free monitoring of biorecognition events. As to gold nanoparticles, SPR is localized at the particle surface, and therefore the use of these LSPR for sensing as in the case of non-planar metal surface is possible. The Mie theory describes that there is a restriction for the movement of electrons through the internal metal framework, when the size of the metal particle is scaled down to nano-level [9]. The collective charge density oscillations of nanoparticles are defined as LSPR. LSPR absorption bands are characteristic of the type of the nanomaterial, the diameter

* Corresponding authors at: Center for Nanobio Integration & Convergence Engineering, National Nanofab Center, KAIST, 291 Daehak-ro, Yuseong-gu, Daejeon 305-701, Republic of Korea. Tel.: +82 42 350 8814; fax: +82 42 350 8800.
E-mail addresses: tjpark@kaist.ac.kr (T.J. Park), leesy@kaist.ac.kr (S.Y. Lee).

0039-9140/$ – see front matter © 2011 Elsevier B.V. All rights reserved.
doi:10.1016/j.talanta.2011.12.021

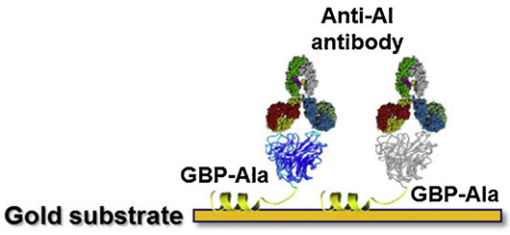

Fig. 1. Schematic diagram of bio-recognition element onto the gold substrate by GBP–fusion proteins. GBP–AIa immobilized on the bare gold surface is sequentially bound by specific interaction between AIa and its anti-AI antibody.

of nanoparticles and their distribution [10]. LSPR-based optical biosensor can be set up without using the specific configurations, for example, the attenuated total reflection optical setup or waveguide coupling. It is possible to fabricate very small devices based on the LSPR technique with a simple optical setup.

With the advances in biosensor technology, many kinds of biosensors based on LSPR have been developed. Using a gold nanoparticle monolayer immobilized on the glass substrate, Okamoto and Yamaguchi has observed the increase of both wavelength and absorbance of the LSPR band as the reflective indices of the sample solutions or the thickness of the films on the surface increased [11]. Developing the biosensor from this technique, Nath and Chilkoti reported an efficient assay for quantify biomolecular interactions in real time on the functionalized surface by measuring the transmission absorption spectra [12]. Moreover, they optimized their chips by investigating the influence of nanoparticle sizes on the sensitivity of the sensors [13]. Another type of LSPR-based biosensor based on triangular silver nanoparticles was developed [14–16]. These silver nanostructures were measured by UV–vis extinction spectroscopy. The determination of organophosphorous pesticides using LSPR has recently been reported by Lin et al. [17]. Chau et al. reported the development of fiber-optic chemical and biochemical probes based on LSPR [18]. Fujiwara et al. measured the binding between the antibodies and proteins using LSPR [19]. Liu et al. recently developed a nanoplasmonic molecular ruler for measuring the nuclease activity and DNA foot printing [20].

However, the device fabrication has been time-consuming and controlling the uniformity in the size of nanometals has been difficult, and resulted in poor reproducibility. For the improvement of these issues, a simple way to excite the LSPR phenomenon was archived by construct a gold-capped nanoparticle array chip. Himmelhaus and Takei have first reported this type of biosensor [21,22]. It depends on the monolayer formation of surface-adsorbed polystyrene spheres, following by the deposition of a thin gold layer on their surface. This LSPR biosensor has demonstrated its linear dependence on the refractive index of the surrounding environment. The shift to the longer wavelength as well as the change in absorbance strength was also observed in the devices as the biomolecules adsorb on the gold surface.

In this work, SPR-based optical biosensor using multi-spot gold-capped nanoparticle array chip for label-free detection of avian influenza (AI) virus as a rapid and user-friendly alternative to conventional techniques is demonstrated. The gold binding polypeptide (GBP)–fusion protein for the AI surface antigen immobilization was immobilized on the gold surface as shown in Fig. 1. Firstly, a bare gold chip was used for immobilization of the GBP–fusion protein, and its specific antibody can be bound subsequently. For enhancing the sensing signals, SPR imaging and LSPR analysis were developed in this study. The multi-spot gold-capped nanoparticle array chip, a LSPR exciting structure, was fabricated by using silica nanoparticles. The optimization as well as characteristics of the LSPR-based optical biosensor was then performed, which brings several advantages such as sensitivity, low-cost and ease to fabrication, and alternatively promises the recent complex optical system in the analysis applications for the dynamic biological interaction.

2. Experimental

2.1. Chemicals and reagents

Restriction enzymes were purchased from New England Biolabs (Berverly, MA, USA). Agarose was from Cambrex BioScience Rockland (Rockland, ME, USA). Unless otherwise stated, all chemical reagents were purchased from Sigma. Ni-NTA spin kit was from Qiagen (Hilden, Germany). All oligonucleotides were synthesized at Genotech (Daejeon, Korea).

2.2. Plasmid construction and protein preparation

Escherichia coli BL21(DE3) ([F$^-$ *ompT hsdS*$_B$ ($r_B^-m_B^-$) *gal dcm* (DE3)], Novagen, Darmstadt, Germany) was used as host strains for general cloning works and gene expression studies. Polymerase chain reaction (PCR) experiments were performed with a PCR Thermal Cycler Mini (Bio-Rad) using High Fidelity PCR System (Takara). Restriction enzymes were purchased from New England Biolabs. DNA sequences of all clones were confirmed by automatic DNA sequencer (ABI Prism model 377, Perkin Elmer).

GBP is for the convenient monitoring of protein immobilization. As described in the previous report, the DNA fragments encoding GBP-fused genes were obtained by overlapping PCR amplification using the plasmid pET-6HGBP containing the 6 histidine and GBP coding gene [23]. The DNA fragments encoding the GBP and the AI viral surface antigen (AIa) were amplified by PCR amplification using the primers P1 (5′-GAAACAGCATATGCACCATCACCATCACCACCACGGCAAAACCCAGGCGACCAG-3′) and P2 (5′-GTACTCGAGGATCGGACGGTTGCTGCCTTTCCAGTTATCACGACAAGACTGAATGGTACCGCT-3′) and the plasmid pET-6HGBP as a template for the construction of 6His-GBP-AIa fusion gene. And then, the PCR product was digested with *Nde*I and *Xho*I, and then cloned into the pET-22b(+) to make pET-6HGBP-AIa.

Recombinant *E. coli* BL21(DE3) strain harboring pET-6HGBP-AIa was cultivated in Luria–Bertani (LB) medium (10 g L^{-1} bactotryptone, 5 g L^{-1} yeast extract and 5 g L^{-1} NaCl) supplemented with 100 μg mL^{-1} of ampicillin at 37 °C and 250 rpm. At the OD_{600} (DU 600 Spectrophotometer, Beckman) of 0.4, cells were induced with 0.1 mM of isopropyl-β-D-thiogalactopyranoside (IPTG, Sigma) for the production of the GBP–fusion protein. After induction, cells were further cultured for 4 h, and harvested by centrifugation at 10,000 × *g* for 10 min at 4 °C. The fusion protein was purified by affinity chromatography using Ni column. Protein concentration was determined by Bradford's method using bovine serum albumin (Sigma) as a standard. The purified proteins were characterized by high-performance liquid chromatography (Agilent) (see Supplementary Information Fig. S1).

2.3. Prediction of putative antigenic regions of H5N1 and H9N2 AI neuraminidase protein

By analyzing the primary structure of H5N1 and H9N2 AI neuraminidase protein obtained from a "chicken and H5N1 neuraminidase structure database" (http://protein.gsc.riken.go.jp/Research/Na/), the putative antigenic regions of envelope protein were predicted. The hydrophilicity, flexible region, antigenicity, and surface probability of H5N1 and H9N2 AI neuraminidase protein were calculated by Kyte–Doolittle plots, Karplus–Schulz prediction, Jameson–Wolf prediction, and Emini prediction, respectively (see Supplementary Information Fig. S2) [24–27].

2.4. Synthesis of specific polyclonal antibodies against AI surface antigen

Rabbit anti-AI polyclonal antibody was prepared from Peptron (Daejeon, Korea). Polyclonal rabbit serum was produced by immunization with a peptide corresponding to the neuraminidase protein residues 291–302 (CRDNWKGSNRPI-NH_2) of H5N1 and H9N2 type AI containing cysteine for conjugation. It was synthesized and conjugated to maleimide-activated keyhole limpet hemocyanin (KLH; Pierce Chemical) by *N*-[4-maleimidobutyryloxy]succinimide ester (GMBS) conjugation method [28], and conjugated to ovalbumin (OVA; 45,000 M_W) which serves as a non-relevant carrier protein for enzyme-linked immunosorbent assay (ELISA). Female rabbits (age 12–22 weeks) were injected 3 times at 21 day intervals with 500 mg of peptide–KLH conjugate in Freund's complete adjuvant (FCA; Pierce Chemical) according to the manufacturer's protocol. Serum was screened by indirect ELISA using the peptide–KLH conjugate. Each well of the 96-microwell ELISA plate was coated with 10% (w/v) of peptide–OVA conjugate in 50 mM carbonate buffer (pH 9.0), and the plates were incubated overnight at 4 °C. Without blocking, 100 μL of antiserum or hybridoma supernatant was incubated for 45 min at 37 °C. Bound antibody was detected with goat anti-rabbit immunoglobulin G (IgG)-horseradish peroxidase and *O*-pheylene-diamine dihydrochloride (Sigma). The titer of the rabbit antiserum following immunization was about 1:100,000. This antibody was purified through the column and concentrated up to 1.6 mg mL^{-1}.

2.5. Binding analysis

The binding of GBP–AIa fusion protein and anti-AI antibody on the gold surface was characterized by using a BIAcore 3000™ SPR system (Biacore). The gold sensor chips, bare gold chip and CM5 amine-coated sensor chip (Biacore), were attached to a separate chip carrier for the easy assembly after surface coating, and was inserted into the SPR system. All experiments were conducted in phosphate-buffered saline (PBS, pH 7.4) at a flow rate of 5 μL min^{-1} at 25 °C, and all sensorgrams were fitted globally using BIA evaluation software. 50 μL of GBP–AIa fusion proteins with various concentrations (6.25, 12.5, 25, and 50 μg mL^{-1}, respectively) were loaded onto the chip using a liquid-handling micropipette. After protein binding, the gold chip surface was washed and equilibrated with PBS solution. For antigen–antibody interaction studies, 50 μL of rabbit anti-AI polyclonal antibodies with various concentrations (1, 2.5, 5, 25, 50, and 100 μg mL^{-1}, respectively) were added to the gold surface, subsequently. In order to determine the optimal binding affinity of GBP–AIa fusion protein and anti-AI antibody to the gold surface, subsequently, all samples were examined with various concentrations by the serial dilution, respectively.

2.6. Surface plasmon resonance imaging analysis

All SPR imaging experiments were performed with an SPR imaging apparatus (SPR*i*, K-MAC, Korea). An incoherent light source (a 150 W quartz tungsten–halogen lamp, Schott) was used for excitation as previously reported [29]. Briefly, *p*-polarized collimated white light incident on a prism/Au/thin film/buffer flow cell assembly was set at a fixed angle. Reflected light from this assembly was passed through a band pass filter centered at 830 nm and collected by a CCD camera (Sony, Japan). The Scion Image Beta 4.0.2 software (Scion Corp., USA) was used to analyze the images.

2.7. Fabrication of multi-spot gold-capped nanoparticle array chip and optical spectroscopy system for influenza diagnosis

For deposition of chromium (Cr) and gold (Au) on the slide glass substrate (S-1215, 76 mm × 26 mm × 1 mm, Matsunami Glass, Japan), a sputtering equipment (MHS 1800, MooHan, Korea) was used at a base pressure of 4×10^{-6} Torr. A Cr layer of 5 nm and bottom Au layer of 40 nm were deposited onto the slide glass substrate. The growth rates were manually adjusted to 0.1 Å s^{-1} (Cr) and 1.0 Å s^{-1} (Au), respectively. The surface of silica nanoparticles was modified using 1% (v/v) 3-aminopropyltriethoxy silan (γ-APTES, Sigma–Aldrich) solution in ethanol by continuous stirring at room temperature for 24 h. The modified silica nanoparticles were then prepared at 1% (v/v) by dispersing in deionized (DI) water. For fabricating the multi-spot biochip, a 60 multi-spot (diameter: 2 mm) silicon–rubber mask was carefully placed on the surface of chromium/gold-deposited slide glass substrate. Then, 1 mM 4,4′-dithiodibutyric acid (DDA, Sigma–Aldrich) was introduced to the gold-layered surface and left for 1 h to allow formation of a self-assembled monolayer (SAM) of the DDA. The previously surface activated silica nanoparticles and 400 mM 1-ethyl-3-(3-dimethylaminopropyl) carbodiimide (EDC, Sigma–Aldrich) were mixed 1:1 and introduced to the activated SAM formation for 1 h. The EDC served to activate carboxyl group of SAM formation, which in turn, formed esters between the amino group of nanoparticles and the carboxyl group of SAM formation. After addition of each solution, the nanoparticle layer modified substrates were rinsed thoroughly with DI water to remove the excess surface-modified nanoparticles and subsequently dried at room temperature. Finally, a top Au layer of 30 nm in height was deposited onto the nanoparticle layer modified substrate using the sputtering equipment. The multi-spot gold-capped nanoparticle array chips were in agreement with the well-known properties that provided a suitable platform for LSPR-based analysis as a previous report [30]. The instruments for the evaluation of the optical properties of multi-spot gold-capped nanoparticle layer chip were based on an LSPR spectroscopy microscopy system (Ocean Optics, USA). Experimental setup for the evaluation of optical properties was reported in our previous studies (see Supplementary Information Fig. S3) [30,31].

2.8. Label-free detection of AI using antigen–antibody interaction on the multi-spot gold-capped nanoparticle array chip

First, an aliquot (5 μL) of 100 μg mL^{-1} GBP–AIa solution was introduced to multi-spot gold-capped nanoparticle array chip and incubated for 1 h. After the immobilization of AIa, the surface of multi-spot chip was rinsed thoroughly with DI water and dried at room temperature. We could immobilize AIa on the surface of multi-spot chip because GBP–fusion protein with AIa could be immobilized on the gold surface of multi-spot chip. A desired concentration of anti-AI antibody was introduced to the GBP-AIa-immobilized multi-spot chip surface, and the inter-reaction was allowed, which was incubating for 1 h at room temperature. After a stringent washing of the surface with DI water, the change in the spectrum was monitored by using a label-free optical biosensor system (see Supplementary Information Fig. S4).

3. Results and discussion

3.1. Binding capability of GBP–fusion protein onto the gold surface

To investigate the sensing window, the concentrations (6.25, 12.5, 25 and 50 μg mL^{-1}) of GBP–AIa fusion protein were varied

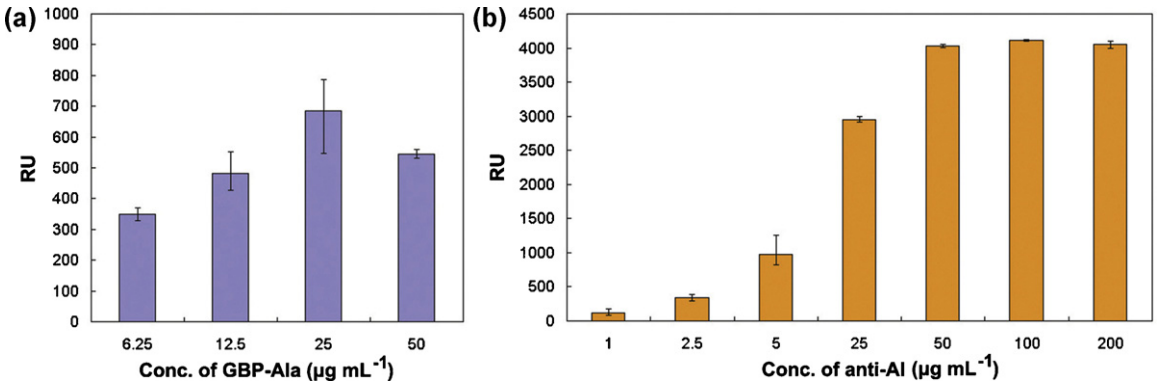

Fig. 2. Molecular binding optimization of GBP–AIa and its antibody with different concentrations. (a) Specific bindings of GBP–AIa antigen on the gold surface with various concentrations (6.25, 12.5, 25, and 50 μg mL^{-1}, respectively). (b) Subsequent bindings of anti-AI antibody with various concentrations (1, 2.5, 5, 25, 50, 100, and 200 μg mL^{-1}, respectively). The bindings were started at 150 s and the unbound samples were washed at 750 s. The more amount of resonance unit (RU) was shown in higher concentration.

and immobilized onto the gold chip surface by SPR microfluidics. A greater shift in resonance unit (RU) was observed by SPR analysis with increasing concentration of immobilized GBP–AIa bound on the planar surface at various concentrations (Fig. 2a). These results suggest that the SPR sensor with GBP–fusion protein implemented on the bare gold surface can be an effective system for biomolecular binding. Thus, the concentration of GBP–AIa was fixed to 25 μg mL^{-1}.

For the subsequent binding of anti-AI antibody, different concentrations (1–200 μg mL^{-1}) of specific antibody were bound to the GBP–AIa fusion protein on the gold sensor chip. The saturated 4000 RU value implies that about 4 ng of anti-AI antibody was immobilized onto the gold surface area of 1 mm^2. One RU is determined as 0.0001° of resonance angle shift and equivalent to a mass change of the 1 pg mm^{-2} on the sensor chip surface [32,33]. Specific anti-AI antibody against AIa was applied to the GBP–AIa-layered surface to monitor specific binding between GBP–AIa and anti-AI by using SPR biosensor (Fig. 2b). However, its limit of detection for anti-AI antibody was 1 μg mL^{-1}, which has a low sensitivity. Therefore, a more sensitive detection tool is needed to enhance signal evaluations of the biosensor.

3.2. Target binding efficiency of immobilized GBP–fusion protein

To verify the significant binding of GBP–AIa and anti-AI rather than by PBS, control experiments were performed. SPR chips were immersed in PBS for 10 min without immobilization of GBP–AIa and anti-AI. No significant RU shift was observed (data not shown). Similarly, the SPR chip immobilized GBP–AIa was immersed in the PBS. Thus, it is confirmed that the cases without specific binding between GBP–AIa and anti-AI antibody do not affect RU shift. In order to investigate the selectivity of antigen–antibody binding, a nonspecific binding experiment using anti-rabbit IgG was carried out. Fig. 3a shows that only the specific anti-AI was selectively bound to GBP–AIa immobilized on the SPR sensor chip surface.

To compare the target protein-binding efficiency, specific antibodies were immobilized on the gold substrate by two different methods: (1) physical adsorption and (2) covalent cross-linking. For physical adsorption, specific antibody solution (5 μM) in PBS (without Tween 20) was loaded onto the cleaned gold sensor substrate at a flow rate of 5 μL min^{-1}. After immobilization, the sensor substrate was washed with 0.1% PBS-T (PBS with 0.5% Tween 20) at 20 μL mL^{-1} until the SPR signal became stable. Covalent cross-linking was performed by amine-coupling on a dextran-coated sensor substrate, CM5, in accordance with the manufacturer's instructions (Biacore). In these two immobilization methods, the number of immobilized specific antibody on the gold sensor substrate was controlled at the same level as that of the bispecific antibody.

To verify the non-specific binding onto the amine-coated gold substrate, physical adsorption and chemical cross-linking of GBP–AIa fusion protein of about 60 resonance units (RU) were observed in SPR response on the CM5 amine-coated sensor chip compared with those between GBP–fusion protein and gold surface as shown in Fig. 3b. Furthermore, almost target molecules could not be bound to the GBP–AIa bioreceptor molecules, because the orientation of biomolecules on this sensor surface cannot be

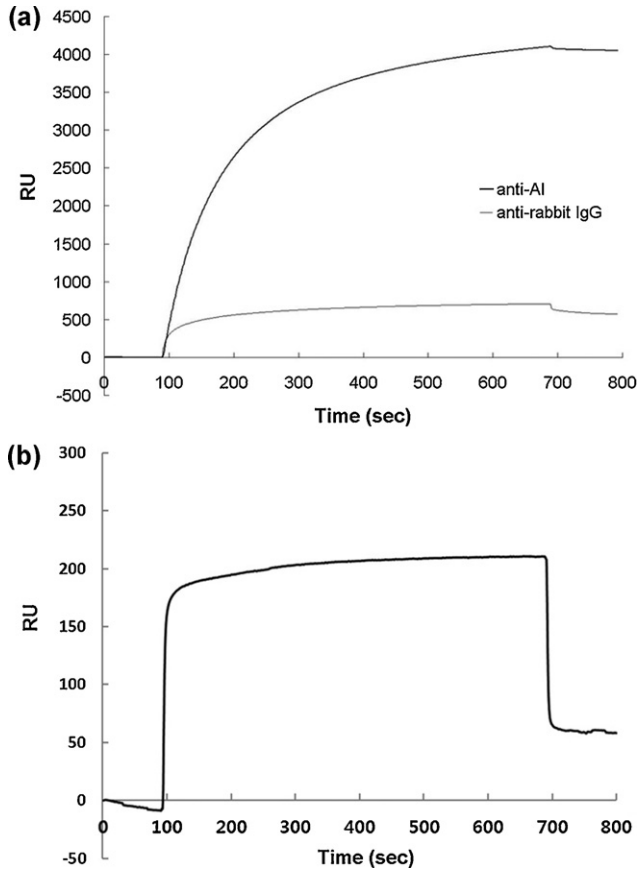

Fig. 3. SPR sensorgrams for (a) specific and selective binding affinity on the bare gold chip and (b) non-specific binding on the amine-coated gold chip with GBP-AIa antigen of 25 μg mL^{-1} fixed concentration. Bold line, anti-rabbit AI antibody of 50 μg mL^{-1}; thin line, anti-rabbit whole IgG of 50 μg mL^{-1}.

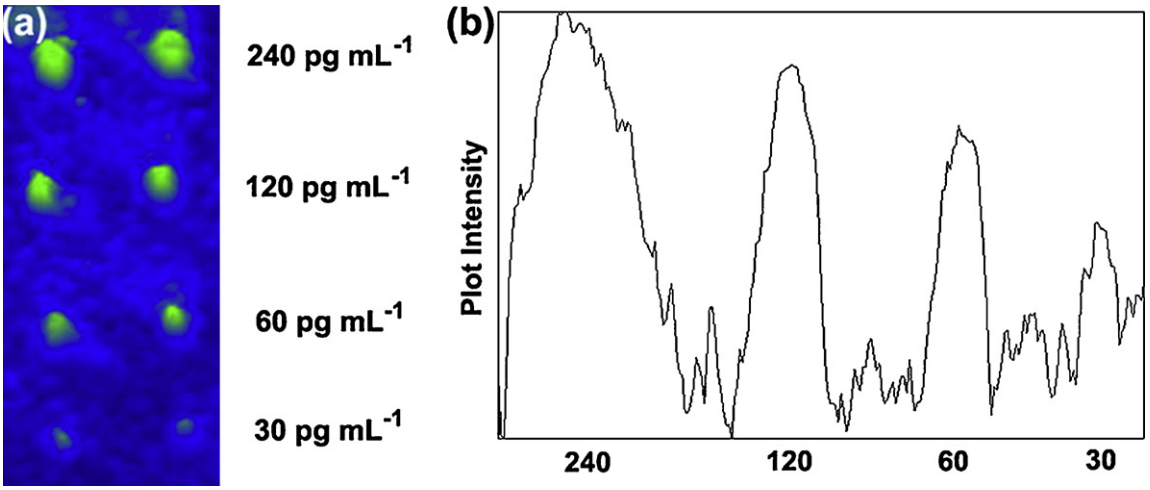

Fig. 4. SPR imaging analysis of GBP–fusion proteins immobilized on the gold substrate having the feature of spray microarrays. (a) Fluorescence image of the sequential binding between GBP–AIa and anti-AI antibody with different concentrations of target molecules. (b) Plot profiles of the immobilized biomolecules scanned through the (a) image of the gold surface.

controlled. From this result, specific immobilization and correct orientation between GBP–fusion protein and gold surface is strong and alternative molecular linker.

3.3. Development of the SPR imaging analysis for enhancing target-bindings

To examine whether the GBP-fusion system can be used for enhancing the sensitivity by using SPR-based protein-protein interaction studies, spray-type microarray and SPR imaging analysis were carried out the following procedure. The GBP–AIa fusion proteins of 25 μg mL^{-1} were immobilized on the bare gold surface by using a piezomicroarrayer. After immobilization of the GBP–AIa fusion proteins, the substrate was incubated in a solution of 0.02% (v/v) Tween 20, 0.1% (w/v) BSA, 50 mM sodium phosphate, and 300 mM NaCl (pH 8.0) for 30 min. Then, the gold substrate was rinsed 3 times with DI water and dried with air condition. Subsequent binding of the anti-AI antibodies with different concentrations to GBP–AIa fusion proteins bound to the gold surface further incubated and washed. After drying, the chip was analyzed with the SPR imaging apparatus for investigating the sensitivity as shown in Fig. 4. The lowest binding signal was 30 pg mL^{-1} via spray-type arrayer and fluorescence signal. Compared with classical SPR analysis, more sensitive detection was possible in SPR imaging method.

3.4. Fabrication of the LSPR chip for enhancing target-bindings

In this study, we fabricated a label-free optical biosensor based on the deposition of a thin gold film on the 60 multi-spot silica nanoparticle array chip with the simple process. The multi-spot gold-capped nanoparticle array chip used the silica nanoparticles as the core and a thin gold film as a cap on the surface (Fig. 5a). The excellent monodispersity of the resulting of commercially available silica nanoparticles translates into the visible region. Especially, the modified silica nanoparticles were formed as a monolayer by covalent attachment using the monolayer of DDA following the deposition of 40 nm gold thin film. The absorbance peak of 60 multi-spot gold-capped nanoparticle array chip was observed at 540 nm as shown in Fig. 5a. This structure can excite the LSPR signal easily with the high reproducibility.

The sensing ability of the 60 multi-spot gold-capped nanoparticle array chip was examined by specific interaction between AI antigen and its antibody. The changes in the LSPR absorbance peak

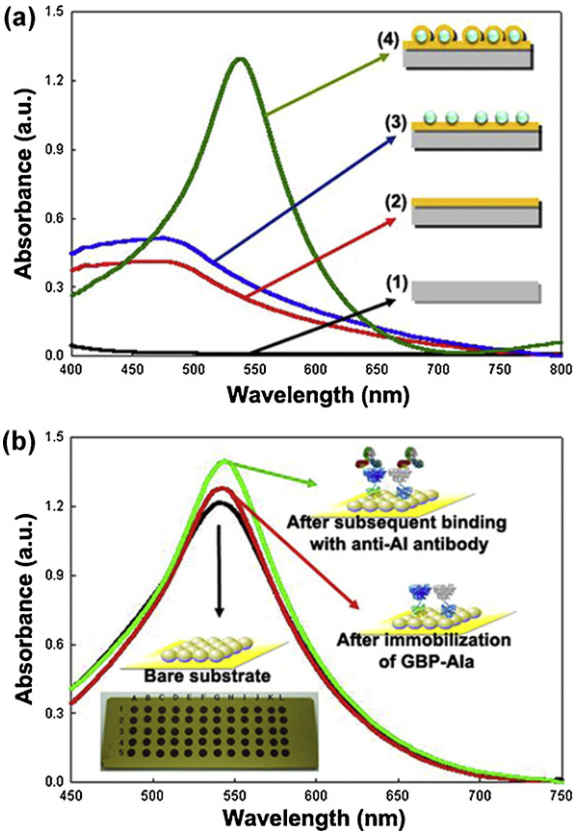

Fig. 5. (a) Optical characteristics of multi-spot gold-capped nanoparticle array chip with LSPR absorbance peak. (1) Slide glass substrate, (2) after gold deposition on slide glass substrate, (3) after silica nanoparticle array on the gold-deposited substrate, and (4) gold-capped nanoparticle array chip. Absorbance peak of multi-spot gold-capped nanoparticle array chip was observed at 540 nm. (b) Absorbance spectrum of LSPR properties obtained after binding of 100 μg mL^{-1} GBP–AIa with 1 μg mL^{-1} anti-AI antibody in wavelength region (from 450 nm to 850 nm). LSPR properties of bare substrate (black line), GBP–AIa-immobilized on the multi-spot chip surface (red line), binding reaction between GBP-AIa and anti-AI antibody on the multi-spot chip surface (green line). Inset represents the 60 multi-spot gold-capped nanoparticle array chip with one spot of 2 mm in diameter. (For interpretation of the references to color in this figure legend, the reader is referred to the web version of the article.)

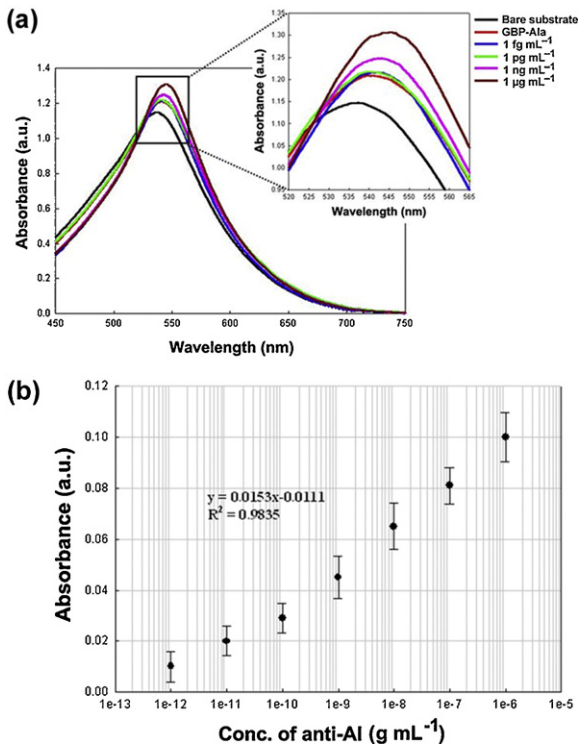

Fig. 6. Optical properties obtained after interaction of AI surface antigen with serial dilutions of anti-AI antibody. (a) Superimposed absorbance spectrum curves obtained from GBP–AIa immobilized on the surface of multi-spot chip in the presence of anti-AI antibody with concentrations ranging from 1 fg mL^{-1} to 1 μg mL^{-1}. (b) Calibration curve for absorbance dependence on anti-AI antibody concentration by using GBP–AIa-immobilized multi-spot chip.

of the multi-spot gold-capped nanoparticle array chip were greatly influenced by the thickness of the biomolecular layers on the chip surface. The absorbance strength increments caused by the formation of several biomolecular layers on the surface were observed for GBP-AI antigen and anti-AI antibody. Fig. 5b shows the superimposed spectrum profiles obtained from 60 multi-spot gold-capped nanoparticle array chip, and the absorbance peak was observed at 540 nm (black line). When GBP-AI antigen of 100 μg mL^{-1} in PBS solution was immobilized on the surface of 60 multi-spot gold-capped nanoparticle array chip, we could observe an increase in the absorbance intensity (red line). Under a similar condition, the interaction condition of 1 μg mL^{-1} anti-AI antibody against the immobilized antigen (GBP–AIa) caused a significant enhancement in the absorbance intensity (green line).

3.5. Sensitivity of biosensor performance

Fig. 6a shows the superimposed absorbance spectrum curves obtained from GBP–AIa antigen immobilized on the surface of 60 multi-spot gold-capped nanoparticle array chip in the presence of anti-AI antibody with concentrations ranging from 1 fg mL^{-1} to 1 μg mL^{-1}, pronounced absorbance increments were observed. The calibration plots in Fig. 6b display the dependence of the absorbance intensity on the concentration of anti-AI antibody. The detection limit of the 60 multi-spot gold-capped nanoparticle array chip was determined as 1 pg mL^{-1} anti-AI antibody with a wide dynamic linear range between 1 pg mL^{-1} and 1 μg mL^{-1} and R^2 value of 0.9835 for Δabsorbance. Error bars correspond to the standard deviation of triplicate measurements (n = 3). The standard deviations of the absorbance intensity value were less than 10% in all the measurements using all the 3 different chips, which indicated that our chips could be fabricated uniformly and are suitable for fabrication of devices with similar responses. Experiments with blood samples toward this goal are currently in progress in the laboratory. A possible disadvantage of our method in comparison to the standard SPR-based analyses might be that our method would not allow studying an unstable biomolecular interaction. However, the sensitivity of the chip by the signal enhancement was very low. Moreover, the GBP–fusion protein binding to the gold substrates is highly specific, and the fusion proteins bound to the gold micro-patterns remained functional as demonstrated by successful antigen–antibody interactions. These results suggested that a strong enhancement of a local signal field was generated around the nanostructure owing to the specific interaction with refractive index in the bio-layers, which have the potential of becoming new widely used tools.

4. Conclusion

In conclusion, we evaluated an optical biosensor system for the influenza detection on the gold surface as a proof-of-concept, which is the flat bare and nano-embossed surface. Signal optimization by the binding of receptor and target using SPR was examined via various concentrations of biomolecules and selective binding of target was tested with whole IgG on the bare gold substrate. For the more sensitive detection, SPR imaging analysis was performed on the piezoarray-type microarray chip. Furthermore, LSPR was performed for highly efficient detection of AI on the nanoparticle-capped array chip. For the detection of protein–protein interactions by integrating the genetically engineered protein employing an SPR, SPRi, and LSPR system, specific and efficient binding of the GBP–fusion proteins on the gold substrates, and the interaction between the GBP–fusion protein and anti-AI antibodies could be demonstrated. Furthermore, the multi-spot gold-capped microarray chip developed in this study can be used for highly sensitive detection of protein interactions. The GBP–fusion protein could be specifically immobilized onto the gold nanoparticles. This optical biosensor system was employed for the successful detection of influenza virus by a spectrum and signal intensity measurement using SPR, SPRi and LSPR system. The specific binding of the GBP–fusion protein onto the gold surfaces suggests that various nanobiosensor devices can be similarly manufactured for the detection of clinical diseases and other protein–protein interactions. These assays will allow high-throughput bioassays of multiple samples. Another obvious advantage of this system is that any protein can be fused to GBP, which can be easily produced by simply cultivating the corresponding recombinant cells. This platform technology should be useful for developing optical biosensors and diagnostic applications for their various advantages such as high sensitivity and specificity, which permits them to rival the most advanced optical protocol. However, a validation of the influenza detection in a practical point of view may need additional works such as real sample test and mixed sample test.

Acknowledgments

This work was supported by the Technology Innovation Program through the Korea Innovation Cluster Foundation funded by the Ministry of Knowledge Economy (No. A2010D-D013) and a grant from the National Fisheries Research and Development Institute (NFRDI, Korea).

Appendix A. Supplementary data

Supplementary data associated with this article can be found, in the online version, at doi:10.1016/j.talanta.2011.12.021.

References

[1] J. Homola, Anal. Bioanal. Chem. 377 (2003) 528–539.
[2] Y. Yao, B. Yi, J. Xiao, Z. Li, ICEEB 2007 (2007) 11043–11046.
[3] R.L. Rich, D.G. Myszka, J. Mol. Recognit. 21 (2008) 355–400.
[4] A. Dhawan, J.F. Muth, Opt. Lett. 31 (2006) 1391–1393.
[5] T.-J. Lin, C.-T. Lou, J. Supercrit. Fluids 41 (2007) 317–325.
[6] O. Esteban, A. Gonzalez-Cano, N. Diaz-Herrera, M.-C. Navarrete, Opt. Lett. 31 (2006) 3089–3091.
[7] Y. He, B.J. Orr, J. Appl. Phys. B 85 (2006) 355–364.
[8] M. Valledor, J.C. Campo, I. Sanchez-Barragan, J.C. Viera, J.M. Costa-Fernandez, A. Sanz-Medel, Sens. Actuators B: Chem. 117 (2006) 266–273.
[9] W.L. Barnes, A. Dereux, T.W. Ebbesen, Nature 424 (2003) 824–830.
[10] R.G. Freeman, K.C. Grabar, K.J. Allison, R.M. Bright, J.A. Davis, A.P. Guthrie, M.B. Hommer, M.A. Jackson, P.C. Smith, D.G. Walter, M.J. Natan, Science 267 (1995) 1629–1632.
[11] T. Okamoto, I. Yamaguchi, Opt. Lett. 25 (2000) 372–374.
[12] N. Nath, A. Chilkoti, Anal. Chem. 74 (2002) 504–509.
[13] N. Nath, A. Chilkoti, Anal. Chem. 76 (2004) 5370–5378.
[14] J. Haes, R.P. Van Duyne, J. Am. Chem. Soc. 124 (2002) 10596–10604.
[15] J.C. Riboh, A.J. Hase, A.D. McFarland, C.R. Yonzon, R.P. Van Duyne, J. Phys. Chem. B 107 (2003) 1772–1780.
[16] J. Haes, R.P. Van Duyne, Anal. Bioanal. Chem. 379 (2004) 920–930.
[17] T.-J. Lin, K.-T. Huang, C.Y. Liu, Biosens. Bioelectron. 22 (2006) 513–518.
[18] L.-K. Chau, Y.-F. Lin, S.-F. Cheng, T.-J. Lin, Sens. Actuators B: Chem. 113 (2006) 100–105.
[19] K. Fujiwara, H. Watarai, H. Itoh, E. Nakahama, N. Ogawa, Anal. Bioanal. Chem. 386 (2006) 639–644.
[20] G.L. Liu, Y. Yin, S. Kunchakarra, B. Mukherjee, D. Gerion, S.D. Jett, D.G. Bear, J.W. Gray, A.P. Alivisatos, L.P. Lee, F.F. Chen, Nat. Nanotechnol. 1 (2006) 47–52.
[21] M. Himmelhaus, H. Takei, Sens. Actuators B: Chem. 63 (2000) 24–30.
[22] H. Takei, M. Himmelhaus, T. Okamoto, Opt. Lett. 27 (2002) 342–344.
[23] S. Zheng, D.-K. Kim, T.J. Park, S.J. Lee, S.Y. Lee, Talanta 82 (2010) 803–809.
[24] J. Kyte, R.F. Doolittle, J. Mol. Biol. 157 (1982) 105–132.
[25] P.A. Karplus, G.E. Schulz, Naturwissenschaften 72 (1985) 212–213.
[26] B.A. Jameson, H. Wolf, Comput. Appl. Biosci. 4 (1988) 181–186.
[27] E.A. Emini, J.V. Hughes, D.S. Perlow, J. Boger, J. Virol. 55 (1985) 836–839.
[28] B.L. Geller, J.D. Deere, D.A. Stein, A.D. Kroeker, H.M. Moulton, P.L. Iversen, Antimicrob. Agents Chemother. 47 (2003) 3233–3239.
[29] T.J. Park, S.Y. Lee, S.J. Lee, J.P. Park, K.S. Yang, K.-B. Lee, S. Ko, J.B. Park, T. Kim, S.K. Kim, Y.B. Shin, B.H. Chung, S.-J. Ku, D.H. Kim, I.S. Choi, Anal. Chem. 78 (2006) 7197–7205.
[30] T. Endo, K. Kerman, N. Nagatani, H.M. Hiepa, D.-K. Kim, Y. Yonezawa, K. Nakano, E. Tamiya, Anal. Chem. 78 (2006) 6465–6475.
[31] S.Y. Yoo, D.-K. Kim, T.J. Park, E.K. Kim, E. Tamiya, S.Y. Lee, Anal. Chem. 82 (2010) 1349–1357.
[32] J. Lahiri, L. Isaacs, J. Tien, G.M. Whitesides, Anal. Chem. 71 (1999) 777–790.
[33] A. Subramanian, J. Irudayaraj, T. Ryan, Sens. Actuators B-Chem. 114 (2006) 192–198.